

Surface coating of a side-chain type polyelectrolyte for endowing perm-selectivity between specific anions to an anion-exchange membrane with a small loss of membrane conductivity

Yan-zhen Shen^{a,b}, Xun-liang Wang^c, Yu-xiang Jia^{a,b}, Meng Wang^{a,b,*}

^aKey Laboratory of Marine Chemistry Theory and Technology, Ministry of Education, email: 819292164@qq.com (Y.-Z. Shen), jiaix76@aliyun.com (Y.-X. Jia), Tel. +86 532 6678 6513, email: wangmeng@ouc.edu.cn (M. Wang)

^bCollege of Chemistry and Chemical Engineering, Ocean University of China, Qingdao, 266100, China

^cThe Institute of Seawater Desalination and Multipurpose Utilization, Tianjin, 300192, China, email: 1105897867@qq.com (X.-L. Wang)

Received 31 May 2017; Accepted 18 October 2017

ABSTRACT

The endowment of perm-selectivity for specific ions will further extend the applications of heterogeneous membrane. In this work, a side-chain type weak cationic polyelectrolyte, PVDF-g-PVP, was synthesized for surface hydrophobization of heterogeneous anion-exchange membrane (AEM) in order to impart perm-selectivity between specific anions with different Gibbs hydration energy. After microstructure observation and chemical composition analyses by SEM, AFM, EA and FTIR, the perm-selectivity between specific anions, electrical resistance, transport number, limiting current density, surface homogeneity, as well as salt permeability of the modified AEMs were investigated. Series of electro dialysis experiments in $\text{SO}_4^{2-}/\text{Cl}^-$ system indicated that a significant perm-selectivity was indeed achieved by the attachment of PVDF-g-PVP coating. In particular, it was worth noting that only a small loss of membrane conductivity was observed after the functionalization. This should be closely related to the micro-phase separation morphology of the coating layer which was induced by the polarity difference between the main chains and side chains of PVDF-g-PVP. Besides, the chronopotentiometric analyses indicated surface homogeneity of the heterogeneous AEM was significantly enhanced and then effectively ameliorated concentration polarization behaviors at the membrane-solution interface. Meanwhile, the perm-selectivity for co-ions was also improved and suppressed back diffusion behaviors of salt driven by concentration gradient. In brief, the modifying scheme proposed in this work can effectively improve comprehensive transport properties of conventional heterogeneous AEM.

Keywords: Anion-exchange membrane; Surface coating; Perm-selectivity; Concentration polarization; Electro dialysis

1. Introduction

It is well known that the electro dialysis technology plays more and more important roles today in the industrial applications for the deionization of aqueous solutions [1]. As the core of the process, ion exchange membranes (IEMs) with some special properties must be developed accordingly to meet new requirements from some practical applications [2]. For example, how to remove harmful ions such

as fluoride and nitrate ions from groundwater and brackish water has attracted much attention in the field of water purification [3–7]. Besides, the separation of SO_4^{2-} from mixtures for avoiding the scale formation in a subsequent industrial process is often expected. Thus, it is clear that the anion-exchange membrane (AEM) with the selective rejection or permeation for some specific anions is badly needed.

Nowadays, various mechanisms for imparting AEMs with perm-selectivity between specific anions have been proposed and practiced, including size-sieving effect by increasing crosslinking degree of AEMs, the differences

*Corresponding author.

in electrostatic interaction between anions and membrane surface by introducing an anionic polyelectrolyte layer as well as their differences in affinity by adjusting hydrophilicity/hydrophobicity of membrane surface [8]. Around the above mechanisms, series of preparation schemes have also been developed, such as adsorption [9,10], coating [11,12] and layer-by-layer assembly [13,14], to attach an oppositely charged layer or a relatively hydrophobic layer to conventional membrane surface. Although the above-mentioned schemes were mostly designed for homogeneous AEMs, some of them have also been extended for the development of special heterogeneous membranes in view of their wide applications in water purification and waste water reclamation. For instance, Kikhavani et al. attempted to prepare a heterogeneous AEM with high selectivity for the nitrate by choosing the hydrophobic polymer (chlorinated polypropylene) as binder and the hydrophobic compound (activated carbon particles) as additive, respectively [15]. In addition, we also immobilized the PEI layer on heterogeneous AEM surface by self-assembly and covalent grafting, respectively, and preliminarily achieved the selective separation effects between anions with different Gibbs hydration energy, such as F^-/Cl^- system and SO_4^{2-}/Cl^- system [16–17]. However, the experimental results indicated that a significant enhancement of electrical resistance seemed to be unavoidable after the above functionalization, particularly for the employment of some weakly dissociated functional groups [18]. In addition, it can be anticipated that the non-conductive inert binders which distributed at the heterogeneous membrane surface must bring some difficulties to achieve a flawlessly modified layer.

It is worth noting that the construction of so-called microphase-separated membrane morphology can facilitate the transport of counter-ions because their mobility and concentration are simultaneously improved in the formed ion nano-channels, which have been confirmed many times by the recent studies on IEMs for fuel cells [19,20]. Moreover, the related experiments have also indicated that a side-chain type polymer which was composed of hydrophobic backbone and hydrophilic side chains will contribute to the formation of the above characteristic membrane structure due to their significant polarity difference. Enlightened by these, a novel weak cationic polyelectrolyte, PVDF-g-PVP, was synthesized and used as coating material to adjust the affinity between AEM and anions with different Gibbs hydration energy in this work. Hopefully, the coating layer prepared from the novel side-chain type copolymer can not only impart the AEM with the perm-selectivity between the specified anions embracing different hydration energies but also facilitate its electro-dialytic transport properties due to the construction of microphase-separated morphology.

2. Experimental section

2.1. Materials

The heterogeneous AEM, a product of Zhejiang Qianqiu Environmental Protection & Water Treatment Co. Ltd. (China), was selected as the base membrane in this study. Meanwhile, the heterogeneous cation-exchange membrane

(CEM) produced by the same company was also employed in the relevant electrochemical characterization experiments. PVDF (FR904) was purchased from Shanghai 3F New Material Co., Ltd. vinyl pyridine (VP) and azodiisobutyronitrile (AIBN) were purchased from Aladdin reagent company and refined before use. Other reagents, such as NaCl, KOH, Na_2SO_4 and N, N-dimethylformamide (DMF) were used directly without further purification. The indicator, Erio-chrome Black T (EBT), was newly prepared and stored at low temperature.

2.1. Synthesis of the PVDF-g-PVP copolymer

The synthetic scheme of PVDF-g-PVP copolymer was shown in Fig. 1. Briefly, the PVDF (100 g) powder was first treated with a KOH solution (2.5 mol/l) at 60°C for 25 min. The precipitate was collected by filtration and then washed several times with deionized water. After being dried at 60°C for more than 48 h, 9.152 g alkaline-treated PVDF was dissolved in 100 ml DMF till a complete dissolution. Subsequently, 15 ml VP and 0.939 g AIBN were added to the above PVDF solution. Along with a continuous mechanical stirring, the radical graft copolymerization reaction proceeded at 70°C for 24 h under N_2 atmosphere. At last, the product was precipitated with ethanol and washed with deionized water to remove the remaining initiators and monomers. At last, the synthesized copolymer was dried fully in a vacuum drying oven at 45°C for 72 h.

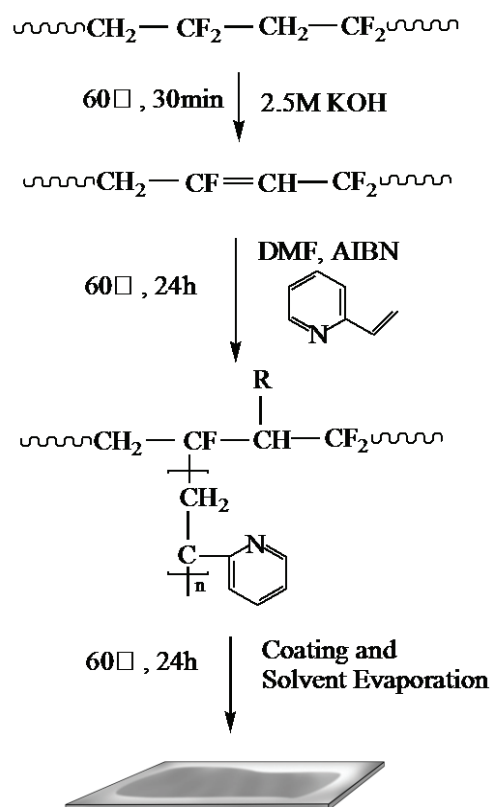


Fig. 1. Schematic diagram of AEM modification process.

2.3. Membrane modification

Specified amounts of PVDF-g-PVP copolymer were dissolved in 100 ml DMF to prepare series of casting solutions with different concentrations, such as 1 wt.%, 5 wt.% and 10 wt.%. After being cured at 50°C for 24 h, the casting solution was coated on the conventional heterogeneous AEM to form a film of 30 μm in thickness. At last, the modified AEM was kept in air for more than 48 h for a complete solvent evaporation and stored in a 0.025 mol/l NaCl solution for subsequent characterizations. For the convenience of narration, the membrane samples were named in this article as follows: A0, the bare AEM; A1, the AEM modified by 1 wt.% PVDF-g-PVP casting solution; A5, the AEM modified by 5 wt.% PVDF-g-PVP casting solution; A10, the AEM modified by 10 wt.% PVDF-g-PVP casting solution.

2.4. Characterization of PVDF-g-PVP copolymer and as-modified AEM

The chemical composition of synthesized PVDF-g-PVP copolymer was investigated by Fourier Transform Infrared Spectra (FTIR, Nicolet iN10 FTIR Microscope) and Elemental Analysis (EA, Vario EL Cube, Elementar). Surface and cross-section morphologies of membrane samples were observed by Field Emission Scanning Electron Microscope (FESEM, Hitachi S-4800). Furthermore, the surface phase behavior of the as-modified AEM was investigated by an Environment Control Scanning Probe Microscope (SPM, SII Nanonavi E-Sweep) using the tapping mode with the silicon cantilever (AN-NSC01) under ambient conditions. In addition, Attenuated Total Reflection-Fourier Transform Infrared Spectra (ATR-FTIR) were also collected for exploring their surface chemical composition by the Nicolet iN10 FTIR Microscope equipped with a smart iTR ATR sampling accessory (germanium crystal, 27°). During the measurements, sixteen scans were taken for each spectrum at a nominal resolution of 4 cm⁻¹.

2.5. Measurements of electrochemical properties

2.5.1. Transport number

The membrane was fastened between two half-compartments into which NaCl solutions with different concentration ($C_1 = 0.5$ mol/L and $C_2 = 0.1$ mol/L) were fed, respectively. Then, the membrane potential can be read from a multimeter by aid of a couple calomel reference electrodes. During the experiments, the solution was circulated in the corresponding compartment by a peristaltic pump (LEAD15-44, Baoding Longer Precision Pump Co. Ltd.) at a flow rate of 300 ml/min to reduce the influence of boundary layer. The measurements were performed at ambient temperature (about 20°C). At last, the transport number can be estimated according to the following equation.

$$E^m = (2\bar{t} - 1) \frac{RT}{F} \ln \frac{\gamma_1 C_1}{\gamma_2 C_2} \quad (1)$$

Here \bar{t} is the transport number of Cl⁻, R is the universal gas constant, F is the Faraday constant, T is the test temperature, and γ is the activity coefficient.

2.5.2. Salt diffusion

The salt diffusion experiments were performed using the method described in our previous paper [21]. The membrane sample (effective area: 3 cm × 3 cm) was fastened between two cells in which 200 ml 1 mol/l NaCl solution and pure water were injected, respectively. During the experiments, two-sided solutions were circulated by a peristaltic pump (LEAD1544, Baoding Longer Precision Pump Co. Ltd.) at a flow rate of 300 ml/min to reduce the influence of diffusion boundary layer formed at membrane-solution interface. As can be imagined, the diffusion of NaCl which is driven by concentration gradient will take place. According to the proportional relation between the conductivity and concentration in a dilute solution, the quantity of the diffused NaCl in the pure water cell can be obtained. Hence, the permeability coefficient (D_s/δ_m) of NaCl can be calculated as follows:

$$\frac{D_s}{\delta_m} = \frac{V \cdot \theta}{S \cdot \Delta c_0} K \quad (2)$$

Here D_s/δ_m is the permeability coefficient of NaCl, D_s is the diffusion constant of NaCl, δ_m is the thickness of membrane, V is the volume of solution, θ is the slope of the linear relation between concentration and conductivity at the pure water side, K is the slope of the linear relation between conductivity and time at the pure water side, S is the membrane area, and Δc_0 is the concentration difference across the membrane.

2.5.3. Current–voltage (I–V) curves

I–V curves were recorded by means of a four-electrode mode in 0.025 mol/l NaCl solution. That is, the electrical current with a stepwise increase was supplied by a potentiostat/galvanostat (DF1731SD2A, Ningbo Zhongce Electronics Co. Ltd.) between a couple of electrodes made of titanium coated with ruthenium. The corresponding steady-state voltage drop values across the membrane sample (effective area: 3 cm × 3 cm) were measured by a multimeter (15B, Fluke Corporation) which was connected with a couple of saturated calomel reference electrodes. In particular, Luggin capillaries were placed closely to membrane surface as much as possible for neglecting the contribution of electrical resistance from solution layer. In order to eliminate the possible influences of the electrode reactions on experimental results, the additional compartments filled with 0.05 mol/l NaCl solution were arranged between the electrode and feed compartments. Before the measurement, all the membrane samples were adequately equilibrated in the test solution for more than 48 h. Besides, no stirring was provided to the test solution during the experiments.

2.5.4. Chronopotentiometry curves

Similar to the equipment used for the measurements of the I–V curves, the chronopotentiometry analyses corresponding to different modification conditions were also performed in a 0.025 mol/l NaCl solution with a current density of about 10 mA/cm². During the experiments, no circulation was exerted to the test solution. When a constant current

density was applied, the voltage drop across the investigated membrane (effective area: 3 cm × 3 cm) was automatically collected every 0.2 s. The changes in conducting fraction (ε) of the AEMs before and after modification can be estimated according to the modified Sand Equation [22].

$$\varepsilon = \frac{2i\tau^{1/2}(\bar{t}-t)}{C_0zF(\pi D)^{1/2}} \quad (3)$$

Here i is the apparent current density; τ is the transition time; t is the transport number of Cl^- in the solution phase; \bar{t} is the transport number of Cl^- in the membrane phase; z is the valence of the ion; D is the diffusion coefficient; C_0 is the concentration of the electrolyte solution.

2.5.5. Perm-selectivity measurements

A series of electro dialysis experiments for $\text{SO}_4^{2-}/\text{Cl}^-$ system were performed to evaluate the perm-selectivity of the membrane samples corresponding to the different modification conditions. In this work, a lab-scale membrane stack was partitioned into electrode compartments, the concentrated compartment and dilute compartment by a piece of the investigated AEM (effective area, 3 cm × 3 cm) and two pieces of CEMs which were alternately arranged between two electrodes made of titanium coated with ruthenium and separated by plexiglas spacers (thickness, 1 cm). Therein, the modified surface of AEM faced the diluted compartment. Initially, the concentrated cell and dilute cell were filled with the same salt solution which was composed of 0.05 mol/l NaCl and 0.05 mol/l Na_2SO_4 . Furthermore, the influences of anion composition in feed solution on the perm-selectivity of the modified AEM between Cl^- and SO_4^{2-} were also investigated. For example, the perm-selectivity coefficients were measured along with the increase of concentration ratio between Cl^- and SO_4^{2-} from 1:1 to 1:10. During the experiments, the salt solution with the same composition was used as the electrode solution for reducing the influence of electrode reactions on the perm-selectivity measurements. The solution was circulated in the corresponding compartment by a peristaltic pump at a flow rate of 300 ml/min. After a 60 min electro dialysis experiment under a constant current density of 10 mA/cm² which was determined on the basis of the limiting current density of the original AEM and a safe factor of 0.85, the concentration of SO_4^{2-} was determined by EDTA complexometry titration using EBT as indicator, and the concentration of Cl^- was determined by potentiometric titration (ZD-2, Shanghai Leici). In addition, the selective separation performance of membrane sample was also investigated under the different concentration ratio between sulfate ion and chloride ion. The perm-selectivity coefficient of SO_4^{2-} against Cl^- can be determined as follows:

$$P_{\text{Cl}^-}^{\text{SO}_4^{2-}} = \frac{t_{\text{SO}_4^{2-}}/t_{\text{Cl}^-}}{c_{\text{SO}_4^{2-}}/c_{\text{Cl}^-}} \quad (4)$$

Here $t_{\text{SO}_4^{2-}}$ and t_{Cl^-} represent the transport numbers of SO_4^{2-} and Cl^- ions, respectively; $c_{\text{SO}_4^{2-}}$ and c_{Cl^-} are the average concentrations (equivalent) of SO_4^{2-} and Cl^- during electro dialysis in the dilute compartment, respectively. The

transport number of the specified anion (SO_4^{2-} or Cl^-) can be defined as the ratio of the current carried by the corresponding anion to the total applied current:

$$t = \frac{F \times V \times \Delta c}{i \times t} \quad (5)$$

In Eq. (5) F is the Faraday constant (96,500 C/mol); V is the volume of the circulated solution; i is the applied current; t stands for the electro dialysis time; Δc is the concentration change of the investigated ion during an electro dialysis process.

3. Results and discussion

3.1. Synthesis of coating materials

In this work, the surface hydrophobization of AEM was carried out to impart the perm-selectivity between anions with different Gibbs hydration energy by the attachment of a weak cationic polyelectrolyte layer. In order to alleviate the influence of the surface modification on membrane conductivity as much as possible, a micro-phase separated structure formed in the modified layer is looked forward, which contributes to the facilitated transportation of counter-ions according to the relevant experimental results about the IEMs for fuel cell. Some public reports have shown that one promising approach to construct the above characteristic membrane morphology is to position the charged groups on side chains grafted onto the hydrophobic main chain [23–27]. Based on the above considerations, the relatively hydrophobic PVDF, a conventional membrane material, and a weakly alkaline monomer, VP, were selected as main chain and side chain, respectively, for the synthesis of the coating material. Herein, dehydrofluorination of PVDF and then the formation of carbon–carbon double bond can be induced by the heated lye treatment, which paved the way for the subsequent graft copolymerization [28–30].

The chemical compositions of alkali-treated PVDF and synthesized PVDF-g-PVP copolymer were investigated by FTIR and compared with that of the pristine PVDF. As can be seen clearly from Fig. 2, they all embraced some

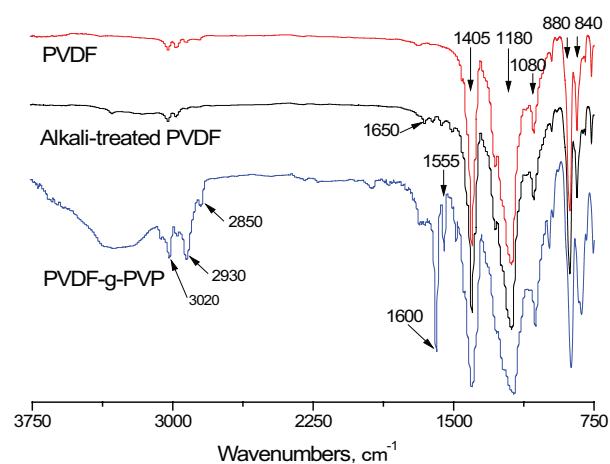


Fig. 2. FTIR spectra of PVDF, alkali-treated PVDF and PVDF-g-PVP.

characteristic peaks, such as C–H stretching at 1405 cm^{-1} , C–F stretching at 1080 cm^{-1} and 1180 cm^{-1} , and amorphous phase at 880 cm^{-1} and 840 cm^{-1} . Besides, some new bands were also observed. For example, a weak absorbance at 1650 cm^{-1} appeared after alkalization treatment, which should be ascribed to the stretching vibration of the C=C double bonds. Moreover, after graft copolymerization with VP, the corresponding spectrum did show two additional peaks at 1555 cm^{-1} and 1600 cm^{-1} , which should be assigned to symmetrical and asymmetrical stretching vibration of C=N, respectively. In addition, in comparison to the spectrum of pristine PVDF, some new peaks at 2850 cm^{-1} , 2930 cm^{-1} and 3020 cm^{-1} were also observed, which should be attributed to stretching vibration of C–H. All these results indicated that the VP has been successfully grafted onto PVDF. At last, the successful synthesis of PVDF-g-PVP was confirmed again by elemental analysis and a grafting degree of about 15% which was defined as the number of VP unit per repeat unit of PVDF was determined.

3.2. The chemical composition and morphology of the modified membrane

After modification, the changes in chemical compositions of membrane surface were also investigated by ATR-FTIR and compared with those of base membrane. As demonstrated in Fig. 3, some new peaks at 1555 cm^{-1} and 1600 cm^{-1} which should be attributed to the stretching vibration of C=N bonds appeared. These showed that the weakly cationic functional groups did distribute at the surface of modified membrane. Interestingly, some characteristic peaks, such as 1465 cm^{-1} and 1720 cm^{-1} which should have belonged to $-\text{CH}_3$ stretching vibration of quaternary ammonium groups and the ester groups of the reinforced polyester cloth of the base membrane, were also observed in the spectrum of modified membrane though their corresponding intensities were reduced to a certain extent. In view of the detection depth of the ATR-FTIR characterization, this indicated that the thickness of the modified layer should be very thin, even less than $1\text{ }\mu\text{m}$.

Subsequently, the surface and cross-section morphologies of the AEMs before and after modification were studied by means of SEM observation. When compared with

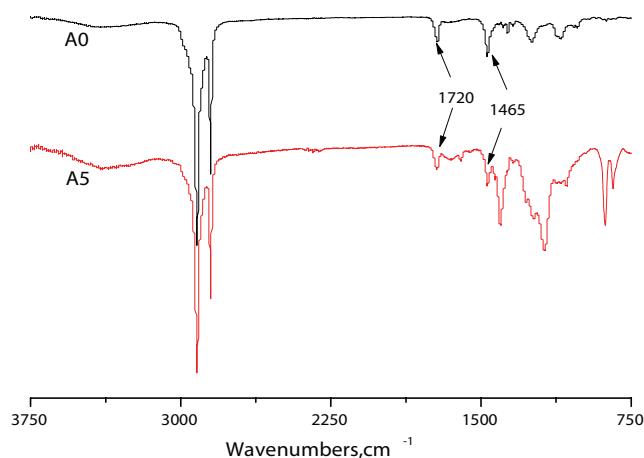


Fig. 3. ATR-FTIR spectra of A0 and A5 membrane samples.

that of the base AEM, it can be noticed from Fig. 4 that a very thin and flat coating layer was indeed attached. On the one hand, the original conductive regions mainly composed of quaternary ammonium groups were covered by the weakly cationic PVDF-g-PVP layer and then the surface hydrophilicity must be reduced, which made the perm-selectivity between specific anions with different Gibbs hydration energy become possible. On the other hand, the inert binders which distributed at membrane surface were also covered by the attached PVDF-g-PVP layer. This may result in a more uniform electric field distribution at the surface of heterogeneous IEM during electro dialysis and then delay the occurrence of concentration polarization.

Furthermore, the micro-phase separated behavior of PVDF-g-PVP layer was investigated by means of AFM. As shown in Fig. 5, the patterns of dark and light were indeed observed. Generally speaking, the hydrophilic domains appear darker in the phase images, whereas the hydrophobic domains appear brighter. Thus, this indicated that the expected micro-phase separation did occur between the stiff hydrophobic main chains and the hydrophilic graft chains of PVDF-g-PVP due to their enthalpy dissimilarities.

3.3. The perm-selectivity of membranes between specific anions

Some anions, such as the scale-forming ions and harmful ions, are often required to a selective removal in the water purification and wastewater reclamation during an electro dialysis process. In view of the significant difference between anions in hydration energy (for examples, SO_4^{2-} , -1000 kJ/mol and Cl^- , -317 kJ/mol) [31], the perm-selectivity between specific anions can usually be carried out by adjusting surface hydrophilicity/hydrophobicity of the AEM. Therefore, a modification scheme by coating a PVDF-g-PVP layer was devised and then evaluated through series of electro dialysis experiments in $\text{SO}_4^{2-}/\text{Cl}^-$ system.

Above all, it was observed from Fig. 6 that the original AEM itself displayed a certain selectivity to Cl^- in this study, which seemed to oppose to a general awareness that the multiply charged ions are preferentially adsorbed by the ion exchange materials. In fact, the different selectivity can even be observed for the same membrane. For example, in Mulyati's work [13], the well-known AMX membrane (Astom Corp., Tokyo, Japan) demonstrated a $P_{\text{Cl}^-}^{\text{SO}_4^{2-}}$ which was greater than 1. On the contrary, in Güler's work [11], the achieved $P_{\text{Cl}^-}^{\text{SO}_4^{2-}}$ of AMX membrane was less than 1. This indicated the selective separation effects also closely related to the electro dialysis conditions besides membrane itself. Therefore, the testing conditions for the perm-selectivity should remain the same for investigating the effects of the weakly cationic coating layers prepared by casting solutions with different concentrations on the perm-selectivity between SO_4^{2-} and Cl^- . As can be seen from Fig. 6, all the perm-selectivity coefficients, $P_{\text{Cl}^-}^{\text{SO}_4^{2-}}$, did significantly decrease after the attachments of the modified layers, which indicated that the expected perm-selectivity was successfully conferred. However, it was also noticed that the perm-selectivity coefficients didn't varied monotonically with the increase of modified solution concentration as expected. Namely, the perm-selectivity was strengthened when increasing the concentration of modified solution from 1 wt.% to 5 wt.%, whereas the perm-selectivity was weakened when continuing to increase it from 5 wt.%

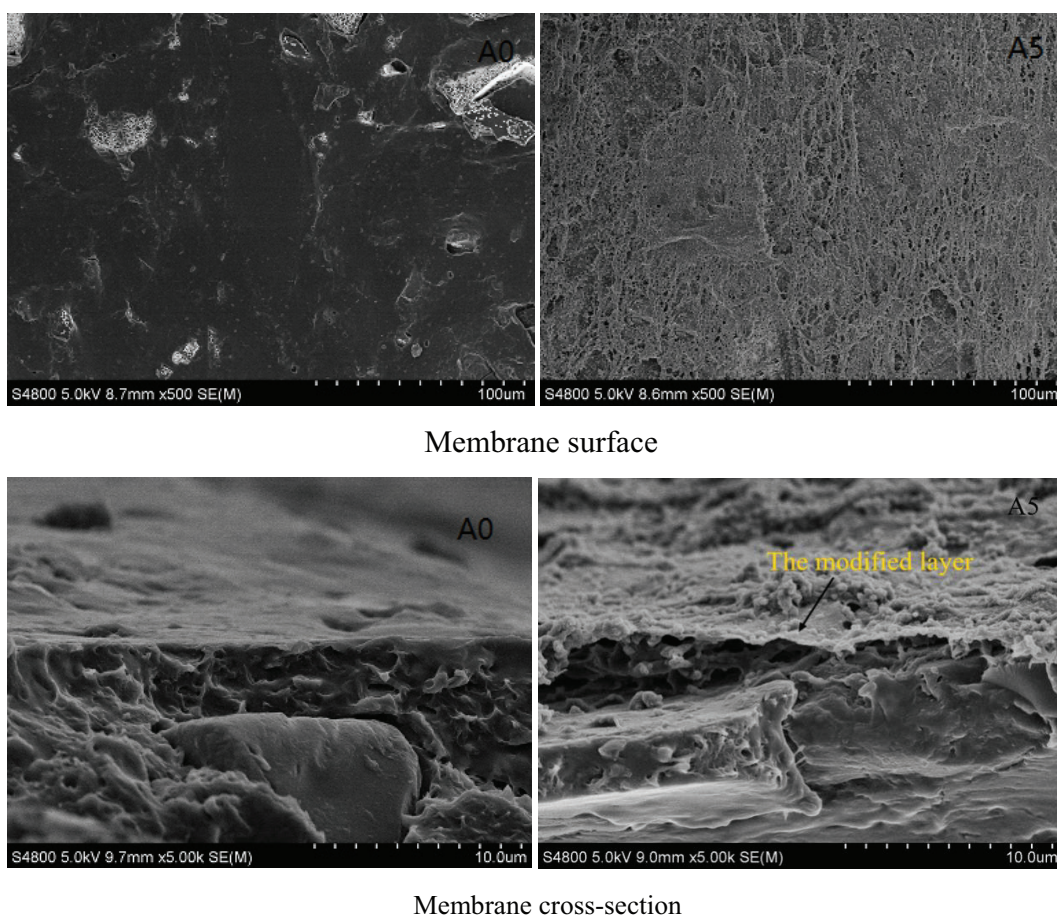


Fig. 4. SEM images of AEMs before and after modification.

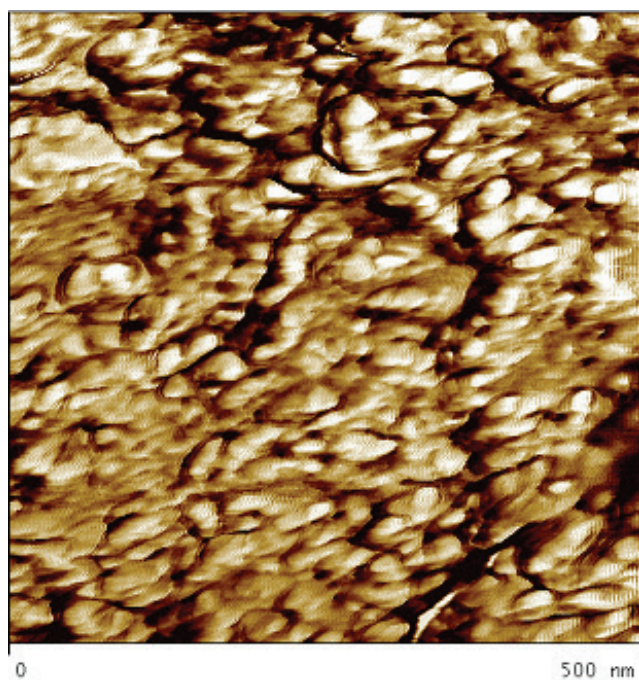


Fig. 5. AFM tapping phase image of PVDF-g-PVP layer.

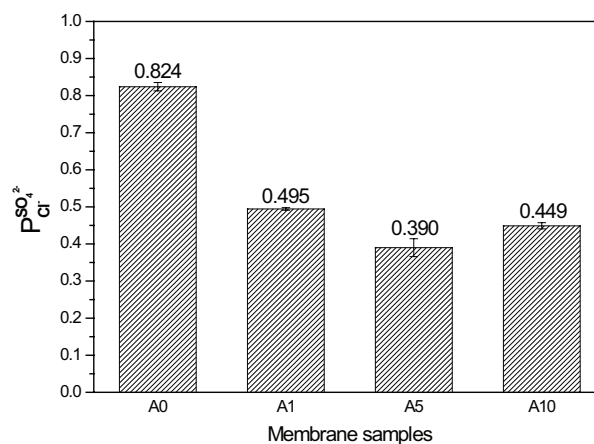


Fig. 6. The perm-selectivity of membranes between SO_4^{2-} and Cl^- corresponding to different modification conditions. (feed solution, $[\text{Cl}^-]/[\text{SO}_4^{2-}] = 1:1$).

to 10 wt.%. The experimental phenomena should be understood as follows: a moderate increase of modified solution concentration can make the modified layer denser, whereas an excessive increase in concentration will result in a significant rise in viscosity of modified solution and then some

flaws appear during the formation of modified layer on the base AEM.

Furthermore, the work performances of the modified AEMs were continuously investigated in a simulated electro dialysis process and compared with those of conventional AEM. It can be seen clearly from Fig. 7 that the concentration ratio of Cl^- to SO_4^{2-} in the concentrated compartments moderately increased with time elapsing when the modified AEM was assembled. This showed that the transport of SO_4^{2-} across the modified AEM was blocked to a large extent and then the separation between Cl^- and SO_4^{2-} can be carried out. In view of the diversity of application background, the influences of anion composition in feed solution on the permselectivity of the modified AEM between Cl^- and SO_4^{2-} were also investigated. As shown in Fig. 8, the perm-selectivity coefficients gradually increased along with the increase in the concentration ratio between Cl^- and SO_4^{2-} from 1:1 to 1:10. The deterioration of perm-selectivity between Cl^- and SO_4^{2-} should be attributed to a higher probability to contact with membrane surface for

SO_4^{2-} than that for Cl^- after the SO_4^{2-} concentration was significantly increased.

3.4. Current–voltage curves

In order to further explore the interfacial transport phenomena taking place at the interface of AEM and solution, I–V curves of AEMs before and after modification were measured. Series of typical I–V curves, including an ohmic region and a pseudo-plateau region, are demonstrated in Fig. 9. In view of the employment of the same test conditions, the changes of membrane electrical resistance induced by the modification operation can be approximately evaluated according to the corresponding slope of the linear part. As can be seen, only a slight increase in electrical resistance (R), less than 6%, was observed. It seemed to be puzzling because the weakly charged PVDF-g-PVP was used as modified material to adjust the hydrophilicity of conventional AEM for a separation between anions with different Gibbs hydration energy in this work. The results may be understood as follows. Above all, it should be partly attributed to the thinness of modified layer which has been confirmed by SEM observations and ATR-FTIR analyses. On the other hand, the possible roles played by its unique micro-phase separation induced by the polarity difference between main chain and side chain should also be taken into consideration. Just as confirmed many times by the

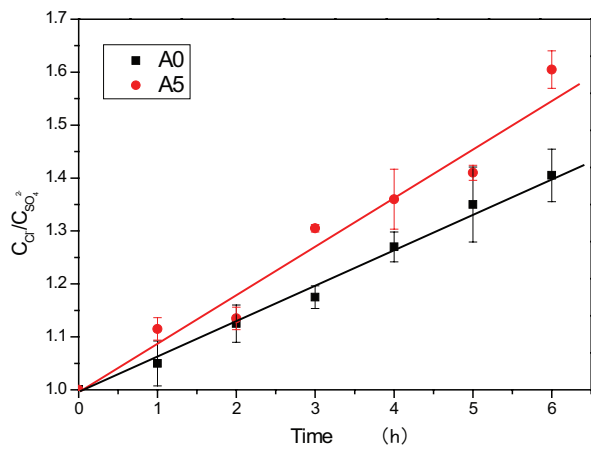


Fig. 7. The changes of ion composition in concentrated compartments with time elapsing.

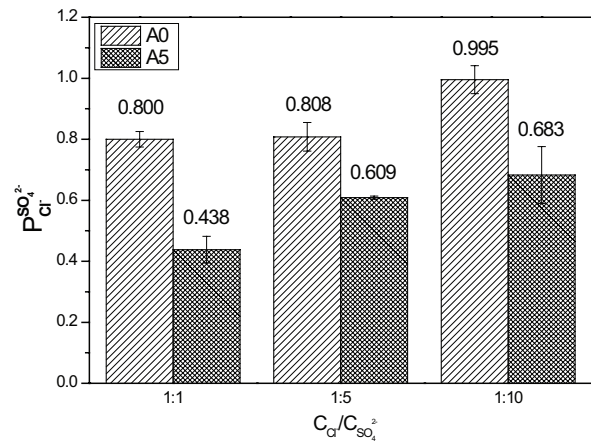


Fig. 8. The perm-selectivity of AEMs between Cl^- and SO_4^{2-} corresponding to different anion composition of feed solution.

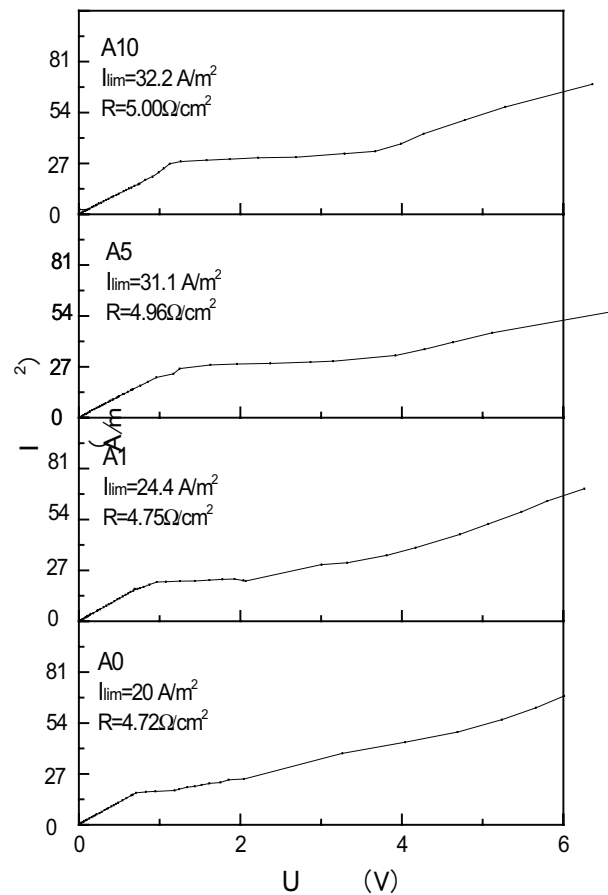


Fig. 9. The I–V curves of AEMs before and after modification.

related studies on IEMs for fuel cells, a microphase-separated membrane morphology contributes to the simultaneous improvements in the mobility and concentration of counter-ions in the formed ion nano-channels and then facilitates their transport.

Moreover, the limiting current density which was traditionally regarded as the maximum current for an economical operation in an electro dialysis process can also be obtained according to the pseudo-plateau region in the I–V curves. Similar to our previous works [16,17], the surface modification of the heterogeneous AEM by the attachment of PVDF-g-PVP polyelectrolyte layer can significantly delay the occurrence of concentration polarization at the AEM-solution interface. As known to all, the heterogeneous membranes usually demonstrate a lower limiting current density than that of the homogeneous one because the existence of non-conductive binders at membrane surface, such as Polyethylene and Polyvinyl chloride, will expedite salt depletion at the conductive regions [32,33]. One can easily imagine that the attached polyelectrolyte layer will contribute to tangential diffusion of anions from the non-conductive regions to the conductive ones and then the ion exhaustion was delayed.

3.5. Chronopotentiometric curves

Subsequently, the chronopotentiometric measurements were also carried out to understand the influences of surface modification performed in this study on the interfacial transport behaviors. As can be seen from Fig. 10, all the chronopotentiometric curves are smooth and the inflection regions are diffuse, which should be the characteristic shape displayed by a heterogeneous membrane. Above all, it was observed that all the initial potentials were almost equal. This confirmed again that there were no significant changes in membrane conductivity before and after modification. In addition, based on the relationships between dE/dt and time, it can be noticed that the transition time which denoted the time taken for the ion depletion at membrane surface to occur after a constant current is applied was remarkably prolonged, for an example, from 23 s of A0 to 44 s of A10. Furthermore, the conducting region fraction increased by 38.3% according to an approximate estimation by the modified Sand equation. This showed that the attachment of polyelectrolyte modified layer did facilitate the tangential transport of ions and then improve surface homogeneity.

3.6. Salt diffusion of AEMs

As known to all, a concentration difference between the diluted and the concentrated compartments will be developed gradually during a practical electro dialysis process. Thus, the back diffusion of electrolyte which is driven by concentration gradient is unavoidable. Without question, this must seriously deteriorate product purity and current efficiency. Therefore, it is necessary to investigate the influences of modification operation performed in this work on the back diffusion behaviors of electrolyte. The NaCl diffusion coefficients of AEMs before and after modification were measured and demonstrated in Fig. 11. It can be noticed that the NaCl diffusion coefficients were

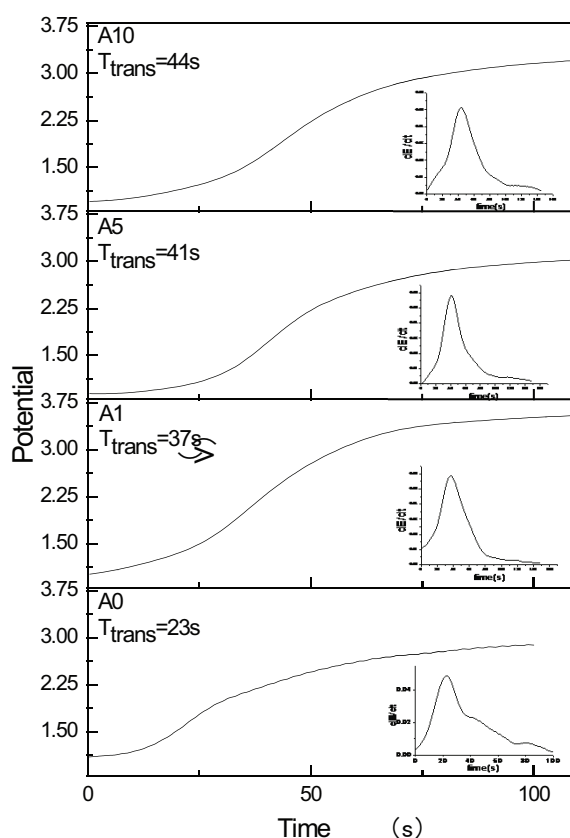


Fig. 10. The chronopotentiometric curves of AEMs before and after modification.

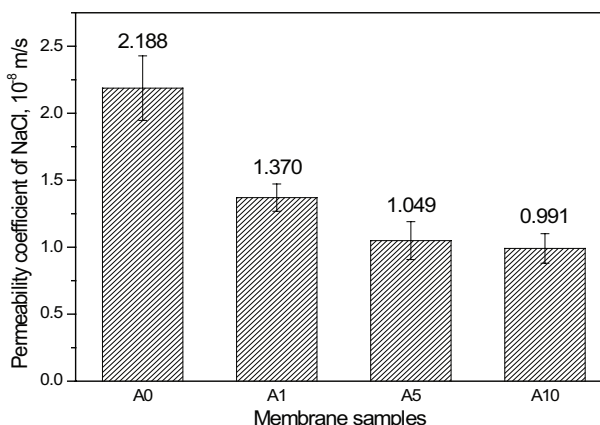


Fig. 11. The diffusion behavior of NaCl through AEMs before and after modification.

significantly reduced after surface modification. Apparently, this should be ascribed to the relatively hydrophobic nature of the PVDF-g-PVP modified layer, which did effectively weaken the affinity between membrane surface and hydrated ions. Besides, the confinement effects in the nano-channel induced by the micro-phase separation in modified layer also contribute to improvements in the perm-selectivity of AEM, which were displayed in Fig. 12.

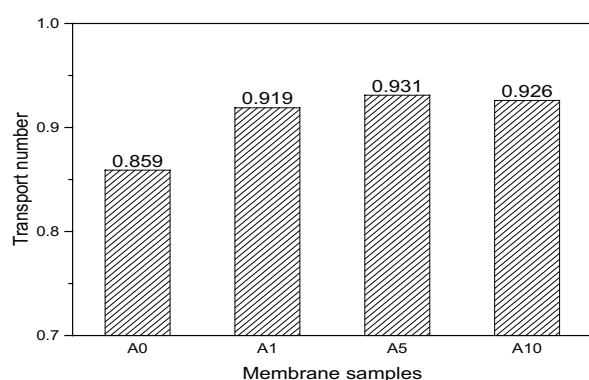


Fig. 12. The Cl⁻ transport number of AEMs before and after modification.

As a result, the ability to block the back diffusion of electrolytes was significantly enhanced after modification.

4. Conclusions

In order to alleviate the trade-off between the special perm-selectivity for anions and membrane conductivity, a side-chain type polymer, PVDF-g-PVP, was synthesized and used for the surface modification of conventional heterogeneous AEM in this work. Series of electro dialysis experiments in the system of Cl⁻/SO₄²⁻ confirmed that the perm-selectivity between the specific anions were indeed achieved through the surface hydrophobization of AEM by coating the weakly alkaline polyelectrolyte. For example, the perm-selectivity coefficient, $P_{Cr}^{SO_4^{2-}}$, decreased from 0.824 to 0.390 before and after modification. Especially, it was worth noting that relatively small loss of membrane conductivity was observed after the above functionality. This indicated the micro-phase separation in modified layer driven by the polarity difference between main chain and side chain of PVDF-g-PVP was conducive to the transport of anions therein. At the same time, it also contributed to the improvement of the perm-selectivity for the co-ions and then effectively impeded back diffusion of electrolyte driven by concentration gradient. In addition, the I-V curves and chronopotentiometric curves showed that surface homogeneity was simultaneously increased and then the occurrence of concentration polarization behaviors at the surface of heterogeneous AEM were significantly delayed. For instance, the conducting region fraction of the conventional heterogeneous AEM increased by 38.3% after being modified according to the proposal put forward in this study. In brief, it is promising to prepare a modified layer from the side-chain type weakly cationic polyelectrolyte for improving the comprehensive transport properties of heterogeneous anion exchange membrane.

Acknowledgments

This research was supported in part by the National Science foundation of China (Nos.21276245 and 21576249) and Key Research and Development Program of Shandong Province (No. 2015GSF117018).

References

- [1] H. Strathmann, A. Grabowski, G. Eigenberger, Ion-exchange membranes in the chemical process industry, *Ind. Eng. Chem. Res.*, 52 (2013) 10364–10379.
- [2] J. Ran, L. Wu, Y.B. He, Z.J. Yang, Y.M. Wang, C.X. Jiang, L. Ge, E. Bakangura, T.W. Xu, Ion exchange membranes: New developments and applications, *J. Membr. Sci.*, 522 (2017) 267–291.
- [3] K. Kesore, F. Janowski, V.A. Shaposhnik, Highly effective electro dialysis for selective elimination of nitrate from drinking water, *J. Membr. Sci.*, 127 (1997) 17–24.
- [4] Z. Amor, B. Bariou, N. Mameri, M. Taky, S. Nicolas, A. Elmidaoui, Fluoride removal of brackish water by electro dialysis, *Desalination*, 133 (2001) 215–223.
- [5] M.A. MenkouchiSahli, S. Annouar, M. Tahaikt, M. Mountadar, A. Soufiane, A. Elmidaoui, Fluoride removal for underground brackish water by adsorption on the natural chitosan and by electro dialysis, *Desalination*, 212 (2007) 37–45.
- [6] N. Kabay, O. Arra, S. Samatya, U. Yuksel, M. Yuksel, Separation of fluoride aqueous solution by electro dialysis: effect of process parameters and other ionic species, *J. Hazard. Mater.*, 153 (2008) 107–113.
- [7] F. Hell, J. Lahnsteiner, H. Frischherz, G. Baumgartner, Experience with full-scale electro dialysis for nitrate and hardness removal, *Desalination*, 117 (1998) 173–180.
- [8] T. Sata, Ion exchange membranes: Preparation, characterization, modification and application, *The Royal Society of Chemistry*, Cambridge, 2004.
- [9] F. Guesmi, Ch. Hannachi, B. Hamrouni, Selectivity of anion exchange membrane modified with polyethyleneimine, *Ionics*, 18 (2012) 711–717.
- [10] M. Amara, H. Kerdjoudj, A modified anion-exchange membrane applied to purification of effluent containing different anions. Pre-treatment before desalination, *Desalination*, 206 (2007) 205–209.
- [11] E. Güler, W. van Baak, M. Saakes, K. Nijmeijer, Monovalent-ion-selective membranes for reverse electro dialysis, *J. Membr. Sci.*, 455 (2014) 254–270.
- [12] M. Vasselbehagh, H. Karkhanechi, R. Takagi, H. Matsuyama, Surface modification of an anion exchange membrane to improve the selectivity for monovalent anions in electro dialysis-experimental verification of theoretical predictions, *J. Membr. Sci.*, 490 (2015) 301–310.
- [13] S. Mulyati, R. Takagi, A. Fujii, Y. Ohmukai, H. Matsuyama, Simultaneous improvement of the monovalent anion selectivity and antifouling properties of an anion exchange membrane in an electro dialysis process, using polyelectrolyte multilayer deposition, *J. Membr. Sci.*, 431 (2013) 113–120.
- [14] S.U. Hong, R. Malaisamy, M.L. Bruening, Optimization of flux and selectivity in Cl⁻/SO₄²⁻ separations with multilayer polyelectrolyte membranes, *J. Membr. Sci.*, 283 (2006) 366–372.
- [15] T. Kikhavani, S.N. Ashrafzadeh, B. Van der Bruggen, Nitrate selectivity and transport properties of a novel anion exchange membrane in electro dialysis, *Electrochim. Acta.*, 144 (2014) 341–351.
- [16] M. Wang, X.L. Wang, Y.X. Jia, X. Liu, An attempt for improving electro dialytic transport properties of a heterogeneous anion exchange membrane, *Desalination*, 351 (2014) 163–170.
- [17] X.L. Wang, M. Wang, Y.X. Jia, B.B. Wang, Surface modification of anion exchange membrane by covalent grafting for imparting permselectivity between specific anions, *Electrochim. Acta.*, 174 (2015) 1113–1121.
- [18] T. Sata, T. Yamaguchi, K. Kawamura, K. Matsusaki, Transport numbers of various anions relative to chloride ions in modified anion-exchange membranes during electro dialysis, *J. Chem. Soc., Faraday Trans.*, 93 (1997) 457–462.
- [19] G.W. He, Z. Li, J. Zhao, S.F. Wang, H. Wu, M.D. Guiver, Z.Y. Jiang, Nano structured ion-exchange membranes for fuel cells: recent advances and perspectives, *Adv. Mater.*, 27 (2015) 5280–5295.
- [20] T.J. Peckham, S. Holdcroft, Structure-morphology-property relationships of non-perfluorinated proton-conducting membranes, *Adv. Mater.*, 22 (2010) 4667–4690.

- [21] T.T. Yao, M. Wang, Y.X. Jia, P.F. Zhou, A modified coating method for preparing a mono-valent perm-selective cation exchange membrane: I. The evolution of membrane property corresponding to different preparing stages, *Desal. Water Treat.*, 51 (2013) 2740–2748.
- [22] J.H. Choi, S.H. Kim, S.H. Moon, Heterogeneity of ion-exchange membranes: the effects of membrane heterogeneity on transport properties, *J. Colloid Interface Sci.*, 241 (2001) 120–126.
- [23] N.W. Li, Q. Zhang, C.Y. Wang, Y.M. Lee, M.D. Guiver, Phenyltrimethyl ammonium functionalized polysulfone anion exchange membranes, *Macromolecules*, 45 (2012) 2411–2419.
- [24] H.S. Dang, E.A. Weiber, P. Jannasch, Poly(phenylene oxide) functionalized with quaternary ammonium groups via flexible alkyl spacers for high-performance anion exchange membranes, *J. Mater. Chem. A.*, 3 (2015) 5280–5284.
- [25] X.M. Wu, W.T. Chen, X.M. Yan, G.H. He, J.J. Wang, Y. Zhang, X.P. Zhu, Enhancement of hydroxide conductivity by the diquaternization strategy for poly (ether ether ketone) based anion exchange membranes *J. Mater. Chem. A.*, 2 (2014) 12222–12231.
- [26] Y.Z. Zhuo, A.L. Lai, Q.G. Zhang, A.M. Zhu, M.L. Ye, Q.L. Liu, Enhancement of hydroxide conductivity by grafting flexible pendant imidazolium groups into poly (arylene ether sulfone) as anion exchange membranes, *J. Mater. Chem. A.*, 3 (2015) 18105–18114.
- [27] X.M. Ren, S.C. Price, A.C. Jackson, N. Pomerantz, F.L. Beyer, Highly conductive anion exchange membrane for high power density fuel-cell performance, *ACS Appl. Mater. Interfaces*, 6 (2014) 13330–13333.
- [28] Y. Zhang, N.L. Le, T.S. Chung, Y. Wang, Thin-film composite membranes with modified polyvinylidene fluoride substrate for ethanol dehydration via pervaporation, *Chem. Eng. Sci.*, 118 (2014) 173–183.
- [29] K.S. Jeong, W.C. Hwang, T.S. Hwang, Synthesis of anionated poly(vinylidene fluoride-g-4-vinylbenzyl chloride) anion exchange membrane for membrane capacitive deionization (MCDI), *J. Membr. Sci.*, 495 (2015) 316–321.
- [30] J. Liu, X. Shen, Y.P. Zhao, L. Chen, Acryloylmorpholine-grafted PVDF membrane with improved protein fouling resistance, *Ind. Eng. Chem. Res.*, 52 (2013) 18392–18400.
- [31] T. Sata, Y. Tagami, K. Matsusaki, Transport properties of anion exchange membranes having a hydrophobic layer on their surface in electro dialysis, *J. Phys. Chem. B.*, 102 (1998) 8473–8479.
- [32] H.J. Lee, M.K. Hong, S.D. Han, S.H. Moon, Influence of the heterogeneous structure on the electrochemical properties of anion exchange membranes, *J. Membr. Sci.*, 320 (2008) 549–555.
- [33] J. Balster, M.H. Yildirim, D.F. Stamatialis, R. Ibanez, R.G.H. Lammertink, V. Jordan, M. Wessling, Morphology and microtopology of cation-exchange polymers and the origin of the overlimiting current, *J. Phys. Chem. B.*, 111 (2007) 2152–2165.